Universal scaling of fluid permeability during volcanic welding and sediment diagenesis

Fabian B. Wadsworth[1]*, Jérémie Vasseur[1], Bettina Scheu[1], Jackie E. Kendrick[2], Yan Lavallée[2], and Donald B. Dingwell[1]
[1]Earth and Environmental Sciences, Ludwig-Maximilians-Universität, Theresienstrasse 41, 80333 Munich, Germany
[2]Earth, Ocean and Ecological Sciences, University of Liverpool, 4 Brownlow Street, Liverpool L69 3GP, UK

ABSTRACT

In sedimentary basins and volcanic edifices, granular materials undergo densification that results in a decrease of porosity and permeability. Understanding the link between porosity and permeability is central to predicting fluid migration in the sedimentary crust and during volcanic outgassing. Sedimentary diagenesis and volcanic welding both involve the transition of an initially granular material to a non-granular (porous to dense) rock. Scaling laws for the prediction of fluid permeability during such granular densification remain contested. Here, based on collated literature data for a range of sedimentary and volcanic rocks for which the initial material state was granular, we test theoretical scaling laws. We provide a statistical tool for predicting the evolution of the internal surface area of a system of particles during isotropic diagenesis and welding, which in turn facilitates the universal scaling of the fluid permeability of these rocks. We find agreement across a large range of measured natural permeabilities. We propose that this result will prove useful for geologists involved in modeling porosity-permeability evolution in similar settings.

INTRODUCTION

Initially granular materials deposited in sedimentary basins commonly densify by compaction and cementation (Fowler and Yang, 1998), and in volcanic systems by viscous processes of compaction and sintering (Quane and Russell, 2005; Wadsworth et al., 2014). These processes in turn significantly change the microstructure and the fluid permeability through the rocks (e.g., Bourbie and Zinszner, 1985; Heap et al., 2015). To date, no effective scaling of the permeability sufficient to describe comprehensively the entire process—from initially granular to finally dense and coherent—has been developed. This limits our ability to model the fluid flow in these systems pertinent to hydrodynamic fracturing efforts in hydrocarbon exploration (Norris et al., 2015), petroleum reservoir migration and storage (Honarpour et al., 1986), volcanic degassing time scales (Edmonds and Herd, 2007), and the propensity of magma to shear fracture (Mueller et al., 2008), amongst many other geological applications. While the trajectory of the porosity-permeability relationship during magma vesiculation is relatively well explored for many of Earth's volcanic systems (Blower, 2001; Klug and Cashman, 1996; Mueller et al., 2005; Saar and Manga, 1999), the evolution of permeability during densification of an initially granular material is less well constrained (Blair et al., 1993; Bourbie and Zinszner, 1985; Martys et al., 1994). A deficit in the scaling efforts addressed herein has been that microstructural controls are rarely explored in detail when global approaches are attempted (e.g., Mueller et al., 2005).

THE GRANULAR TO NON-GRANULAR TRANSITION IN MAGMAS AND SEDIMENTS

Magmas readily fragment to form granular materials (volcanic ash) upon rapid decompression (Alidibirov and Dingwell, 1996), or more generally when local strain time scales approach the structural relaxation time scale of the liquid (Dingwell and Webb, 1989), leading to the generation of in situ and proximal volcaniclastic deposits. Fragments are also deposited in clastic sedimentary processes. Such fragments, sedimentary or volcanic, are variably packed in granular beds which experience changes in fluid flow, pressure, and temperature, and undergo diagenesis or welding, densifying at the expense of pore space (Bourbie and Zinszner, 1985; Fowler and Yang, 1998). This densification also commonly occurs within volcanic interiors where fragmented magma is deposited in cracks within the still-ductile magma itself (Tuffen and Dingwell, 2005) or in subaerial volcanic basins (Branney and Kokelaar, 1992) where fragmental volcaniclastic deposits may remain hot enough to relax viscously (Dingwell and Webb, 1989) and to undergo densification by sintering (Wadsworth et al., 2014). Both of these processes—sediment compaction and viscous sintering—involve the time-dependent evolution of porosity, ϕ, and permeability, k, that accompanies the material transition from a packed granular state through a denser, coherent porous state to an impermeable, fully densified state (Fig. 1). This impermeable state is typically described in terms of the attainment of a percolation threshold, ϕ_c, at which the pores become isolated. For systems undergoing bubble nucleation, growth, and coalescence in a liquid, percolation thresholds of $0.2 \lesssim \phi_c \lesssim 0.7$ have been documented (Blower, 2001; Klug and Cashman, 1996; Mueller et al., 2005; Okumura et al., 2008; Westrich and Eichelberger, 1994). In contrast, during isotropic densification of particles, the percolation threshold can be much lower with $\phi_c \approx 0.03$ (Rintoul, 2000). This wide range in threshold values implies that densifying, initially granular systems are capable of maintaining permeable pathways to very low porosities.

Understanding how permeability evolves during the granular densification process will help us to better understand fluid pressurization that can lead to fracturing. In sedimentary basins, unexpectedly high pore fluid pressures can cause operational failure during exploration drilling,

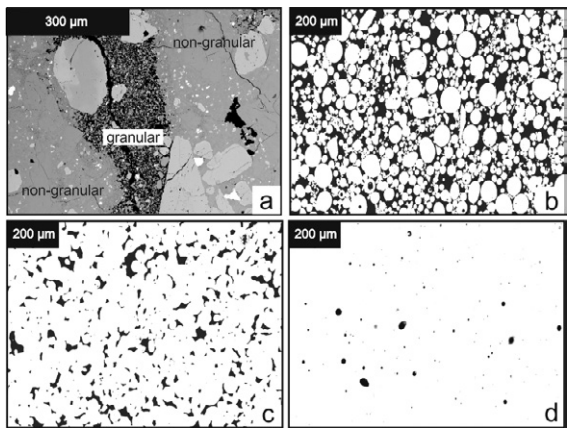

Figure 1. Scanning electron micrographs of granular to non-granular materials. A: Margins of granular-filled cracks in andesite from Volcán de Colima, Mexico, showing granular material sintered to wall of more dense, non-granular host magma (samples from J. Kendrick, 2015, personal commun.). B–D: Variably sintered glass beads, used as analogue for both sandstone diagenesis (Blair et al., 1993) and sintering of volcanic ash (Wadsworth et al., 2014). D: Sintered glass beads at percolation threshold ϕ_c = 0.03. In all images, pores appear black whereas crystals and glass show as gray to white.

*E-mail: Fabian.wadsworth@min.uni-muenchen.de

by drill-hole collapse (Fowler and Yang, 1998). Similarly, in volcanoes, it is the time scales and pressures associated with outgassing-welding processes that are thought to most readily influence eruption likelihood (Quane and Russell, 2005). In silicic crystal-poor volcanoes, the majority of shallow outgassing is thought to occur through cracks filled with densifying hot volcanic ash. This may be the primary degassing mechanism in obsidian-forming magmas (Castro et al., 2014). The efficacy of fluid pressure equilibration through permeable outgassing is a critical parameter in the assessment of whether or not explosive eruption or borehole collapse will occur. The initially granular nature of these in-conduit deposits renders the scaling laws proposed for vesiculation processes inappropriate for the processes of interest to us in this study.

While measurements of fluid permeability in granular sediments undergoing densification are reasonably common (Blair et al., 1993; Bourbie and Zinszner, 1985), those made on initially granular volcanic rocks have only recently become the subject of research (Heap et al., 2015; Okumura and Sasaki, 2014; Wright and Cashman, 2014). In both cases, data from the experimental densification of granular material and quantification of resultant permeability changes are somewhat sparse. Here, we collate a range of permeability data that involve this granular to non-granular transition in volcanic and sediment-derived rocks (Fig. 2) and find a universal scaling. This scaling, when coupled with existing kinetic laws for the evolution of porosity (Fowler and Yang, 1998; Quane and Russell, 2005; Wadsworth et al., 2014), yields the promise of providing predictive tools for the time scales of permeability loss in surficial environments.

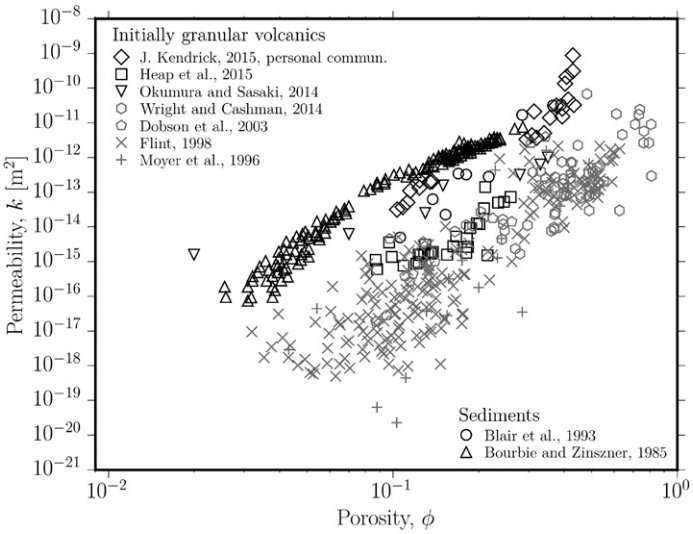

Figure 2. Bulk porosity and permeability of samples that underwent granular to non-granular transitions during volcanic welding or sedimentary diagenesis. Data in black are associated with sufficient information for subsequent analysis.

UNIVERSAL SCALING FOR FLUID PERMEABILITY

Scaling relationships used to define fluid permeability in vesiculating systems commonly require knowledge of the fluid pathway tortuosity or pore-throat length scale (Blower, 2001; Klug and Cashman, 1996; Le Pennec et al., 2001), whereas the length scale best suited to scaling the permeability in granular systems is the particle size. However, in densification scenarios where the system qualitatively evolves from granular toward fully dense (Fig. 1), a universal prediction of k is hampered by a lack of continuous description of the microstructural length scale involved. For models of compaction in sedimentary basins, the simplest power-law form is most commonly used: $k = k_r (\phi / \phi_r)^b$, where ϕ is the porosity, r denotes reference (e.g., the initial) values, and b can range from 2 (Connolly et al., 2009; von Bargen and Waff, 1986) to ~8 (Fowler and Yang, 1998). However, the reference $k_r(\phi_r)$ depends on parameterization of the particle sizes and initial packing, which are not functionally constrained and thus not universal. The most commonly used empirical scaling for the permeability when fluid flow is around spherical particles (granular system) is the Kozeny-Carman relation $k = \phi^3/2s^2$ (e.g., Scheidegger, 1963), where s is the specific surface—the ratio of pore surface area to sample volume—such that the particle length scale can be used to predict s. Adaptations of this scaling are frequently used in models of melt extraction from the asthenospheric mantle (Connolly et al., 2009; McKenzie, 1984). These approaches have been widely applied. Yet they have failed to prove universal, even for idealized geometries (Martys et al., 1994). An easily implemented universal model is the one proposed by Martys et al. (1994), who suggested that k is related to s via:

$$k = \frac{2\phi_*}{s^2}\left(\phi - \phi_c\right)^b, \quad (1)$$

for which $\phi_* = 1 - (\phi - \phi_c)$ and b is 4.2 and may prove to be related to the initial particle geometry. We can calibrate the utility of Equation 1 using samples of sandstone and of sintered glass beads (Blair et al., 1993) for which all of the relevant parameters are measured quantities. This produces reasonable agreement over a large range of both k and ϕ when $\phi_c \approx 0.03$ (Fig. 3, inset). The value of $\phi_c \approx 0.03$ is in excellent agreement with universal predictions for ideal spheres undergoing densification (Rintoul, 2000). For the majority of both sediments and variably welded volcanic rocks, the value of s is unmeasured. Below, we tackle this deficit by estimating how s evolves with ϕ in densifying granular systems.

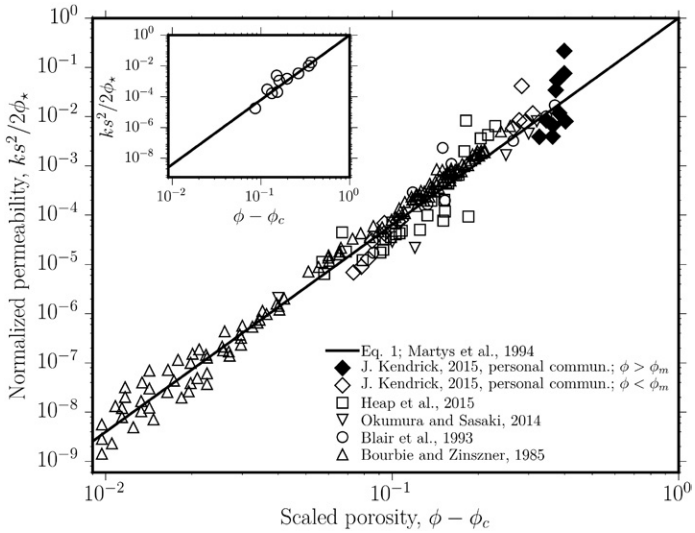

Figure 3. Universal scaling of fluid permeability in rocks across the granular to non-granular transition (via Equation 1) using either measured *s* (specific surface, ratio of internal surface area to sample volume) or, if unknown, calculated -evolution of *s* during densification (using Equations 2 and 3) showing good agreement without any fitting parameters ($r^2 = 0.96$) over a large range of normalized permeability [*k*—permeability; ϕ—porosity; ϕ_c—percolation threshold; $\phi_* = 1 - (\phi - \phi_c)$; ϕ_m—maximum packing porosity of particles]. Inset: Data from Blair et al. (1993) for which *s* was measured directly by image analysis.

PREDICTING THE SPECIFIC SURFACE DURING DENSIFICATION

In order to use Equation 1 effectively, we need to know how s varies from an initial state as ϕ decreases during volcanic welding or sediment compaction. To do this, we use a statistical approach for heterogeneous

granular materials developed by Torquato (2013) who provided solutions for (1) the size of pores between packings of spherical hard particles, and (2) the specific surface of packings of spheres that can overlap with one another randomly, termed overlapping, or that are "hard" and do not overlap, termed non-overlapping. For a given initial value of ϕ and an initial characteristic monodisperse particle radius R (a polydisperse solution is provided in the GSA Data Repository[1]), we can compute the characteristic or "effective" pore radius a that is nestled between the particles, assuming all particles are initially non-overlapping, by starting from the cumulative probability density function $F(x)$ of the pore size where $x = a/R$ and $\beta = 1 + x$:

$$F(x) = \exp\left[(\phi - 1)\left(y_0\beta^3 + 3y_1\beta^2 + 12y_2\beta + y_3\right)\right]. \quad (2)$$

Here y_0, y_1, y_2 and y_3 are parameters that depend on ϕ (given in the Data Repository). The n^{th} moment of the probability density function of x (termed $\langle x^n \rangle$) is then related to the cumulative probability density function $F(x)$ by integrating $\langle x^n \rangle = n\int_0^\infty x^{n-1}F(x)\,dx$. Thus, the mean (i.e., $n = 1$) pore radius, which we take as the characteristic size, is given by $a = R\langle x \rangle$.

Finally, we can use this value of a to compute the specific surface that would exist during densification assuming all of the pores interstitial to the densifying material remain overlapping:

$$s(a) = -\frac{3(1-\phi)\ln(1-\phi)}{a}. \quad (3)$$

The overlapping assumption for the pore space is valid as pores readily interact and are not hard spheres, unlike the initial particles. The exception to the use of Equation 3 is for material that is granular and below the maximum packing porosity of the particles ϕ_m, such as is the case for the high-ϕ experimental portion of our data sets in which particles have only undergone incipient sintering (Table 1). For these data, we compute the surface area directly from the monodisperse R by the simpler geometric relationship $s(R) = 3(1 - \phi)/R$. Using this for the data from experiments using crushed volcanic ash from Volcán de Colima, Mexico (J. Kendrick, 2015, personal commun.), yields an estimation of $\phi_m \approx 0.32$ for these angular, polydisperse particles.

Using Equations 2 and 3 to compute s for use with Equation 1 provides us with tools to assess the scaling of the permeability for natural samples that were initially granular and for which we have constraint of the initial particle size R. The initial values of ϕ are taken as the highest measured value, and, in order to minimize the assumptions made, only data for which the initial characteristic R is quoted are used. The measured values of R and computed a and ϕ_c are quoted in Table 1. Figure 3 shows the results of this scaling coupled with the results for the calibration scaling (Fig. 3, inset). We find good agreement ($r^2 = 0.96$) across many orders of magnitude of normalized permeability. In the Data Repository, we provide this scaling for other combinations of overlapping and non-overlapping particles and pores to show that these work less effectively than the method presented here ($0.56 < r^2 < 0.93$).

DISCUSSION

The scaling presented here can be used to predict a granular system permeability when ϕ and s are measured (Equation 1). Alternatively, knowledge of R of the initial granular system permits the use of these tools to estimate s (Equations 2 and 3) and thus k easily. The conceptual framework developed here is novel because the definition of the length scale used to estimate s changes from R to a as the system crosses below $\phi = \phi_m$ upon deposition and densification, which is when the particles are sufficiently closely packed to be considered densifying in a bed ($\phi < \phi_m$) and not depositing from dispersion ($\phi > \phi_m$).

Despite the progress made using this method, caveats to our approach nonetheless remain and these are important to state explicitly. First and foremost, our proposed scaling does not address anisotropy of the permeability, which can develop during compaction of both sediments and volcanic ash (Wright and Cashman, 2014). Secondly, we treat the particles and the inter-particle effective pores as spherical and quasi-monodisperse (we provide polydisperse solutions for s in the Data Repository). Despite these implicit assumptions, from the apparent efficacy of the present scaling approach, we are led to infer that, for the wide range of samples tested (Table 1), particle angularity or polydispersivity do not have a first-order effect on the inter-particle fluid permeability. The dominant effect of angularity might be on the initial porosity (i.e., the maximum packing density of the particles at deposition), which will in turn impact the permeability and is captured by the bulk ϕ in Equation 1.

Our model carries the implication that it is the processes that affect R (and thus s; Equations 2 and 3) during particle formation, such as the fragmentation conditions (Fowler et al., 2010), bulk composition, and crystal content (Rust and Cashman, 2011), that play an important role in the permeability of the resultant deposits and their evolution during diagenesis or welding. This inference holds the potential of providing an explicit physical link between the bulk isotropic permeability and the mechanisms that control the development of the microstructural elements that are deposited. We conclude that a well-constrained state of the initial isotropic granular system appears to be sufficient to estimate the evolution

[1]GSA Data Repository item 2016065, alternative scaling arguments, is available online at www.geosociety.org/pubs/ft2016.htm, or on request from editing@geosociety.org or Documents Secretary, GSA, P.O. Box 9140, Boulder, CO 80301, USA.

TABLE 1. SUBSET OF THE GEOLOGICAL PERMEABILITY DATABASE FOR WHICH *R* OR *s* IS MEASURED (FIG. 3)

Reference	*R* (μm) measured	*a* (μm); Equations 2 and 3	Percolation threshold ϕ_c	Data type	Comments and sample details
Volcanic materials					
J. Kendrick (2015, personal commun.)	100 (angular)	14.5	~0.03	Experimental	Crushed andesite from the 2012 lava dome at Volcán de Colima (Mexico)
Okumura and Sasaki (2014)*	75.0; 250 (angular)	8.02; 26.7	~0.03	Experimental	Wadatouge (Japan) rhyolitic obsidian
Heap et al. (2015)	25.0 (angular)	1.80	~0.03	Natural	Variably welded block-and-ash flow deposits from Mount Meager (Canada)
Sediments					
Bourbie and Zinszner (1985)	250 (sub-spherical)	20.4	~0.03	Natural	Fontainebleau (France) sandstone; well sorted, ~100 vol% quartz
Blair et al. (1993)#	—	—	~0.03	Natural and experimental	Sintered spherical glass beads and natural sandstones

Note: R—particle radius; *s*—specific surface; *a*—pore radius.
*Two different grain sizes are used in Okumura and Sasaki (2014); we take the lower value of the distribution.
#*s* is measured and Equation 1 can be used directly, so no constraint of *R* or *a*(ϕ) is necessary.

of isotropic permeability during densification by compaction of a sediment bed or by welding in volcanic interiors or ignimbrites (Fig. 3).

CONCLUSIONS

Initially granular materials undergoing densification evolve in terms of microstructure. These microstructural changes affect the bulk porosity and the permeability. We present a universal scaling between a normalized isotropic permeability and the porosity, using relatively few, easily obtainable, measured parameters. We calibrate this scaling using well-characterized materials before estimating its applicability to the literature data available. This scaling provides a tool to predict the fluid permeability across a wide range of porosities, invaluable for fluid flow modeling during volcanic degassing through granular filled cracks and in evolving sedimentary basins.

ACKNOWLEDGMENTS

We acknowledge support from the European Union's seventh program for research and technology under grant agreement VUELCO (282759) and European Research Council grants EVOKES (247076) and SLiM (306488). Comments from Bob Holdsworth, Heather Wright, and two anonymous reviewers greatly improved the clarity of our work.

REFERENCES CITED

Alidibirov, M., and Dingwell, D.B., 1996, Magma fragmentation by rapid decompression: Nature, v. 380, p. 146–148, doi:10.1038/380146a0.

Blair, S., Berge, P., and Berryman, J., 1993, Two-point correlation functions to characterize microgeometry and estimate permeabilities of synthetic and natural sandstones: Lawrence Livermore National Laboratory Technical Report UCRL-LR-114182, 31 p., doi:10.2172/10182383.

Blower, J., 2001, Factors controlling permeability–porosity relationships in magma: Bulletin of Volcanology, v. 63, p. 497–504, doi:10.1007/s004450100172.

Bourbie, T., and Zinszner, B., 1985, Hydraulic and acoustic properties as a function of porosity in Fontainebleau sandstone: Journal of Geophysical Research, v. 90, p. 11,524–11,532, doi:10.1029/JB090iB13p11524.

Branney, M., and Kokelaar, P., 1992, A reappraisal of ignimbrite emplacement: Progressive aggradation and changes from particulate to non-particulate flow during emplacement of high-grade ignimbrite: Bulletin of Volcanology, v. 54, p. 504–520, doi:10.1007/BF00301396.

Castro, J.M., Bindeman, I.N., Tuffen, H., and Schipper, C.I., 2014, Explosive origin of silicic lava: Textural and δD–H_2O evidence for pyroclastic degassing during rhyolite effusion: Earth and Planetary Science Letters, v. 405, p. 52–61, doi:10.1016/j.epsl.2014.08.012.

Connolly, J.A., Schmidt, M.W., Solferino, G., and Bagdassarov, N., 2009, Permeability of asthenospheric mantle and melt extraction rates at mid-ocean ridges: Nature, v. 462, p. 209–212, doi:10.1038/nature08517.

Dingwell, D.B., and Webb, S.L., 1989, Structural relaxation in silicate melts and non-Newtonian melt rheology in geologic processes: Physics and Chemistry of Minerals, v. 16, p. 508–516, doi:10.1007/BF00197020.

Dobson, P.F., Kneafsey, T.J., Hulen, J., and Simmons, A., 2003, Porosity, permeability, and fluid flow in the Yellowstone geothermal system, Wyoming: Journal of Volcanology and Geothermal Research, v. 123, p. 313–324, doi:10.1016/S0377-0273(03)00039-8.

Edmonds, M., and Herd, R.A., 2007, A volcanic degassing event at the explosive-effusive transition: Geophysical Research Letters, v. 34, L21310, doi:10.1029/2007GL031379.

Flint, L.E., 1998, Characterization of hydrogeologic units using matrix properties, Yucca Mountain, Nevada: U.S. Geological Survey Water-Resources Investigations Report 97-4243, 64 p.

Fowler, A.C., and Yang, X.-S., 1998, Fast and slow compaction in sedimentary basins: SIAM (Society for Industrial and Applied Mathematics) Journal on Applied Mathematics, v. 59, p. 365–385, doi:10.1137/S0036139996287370.

Fowler, A.C., Scheu, B., Lee, W.T., and McGuinness, M.J., 2010, A theoretical model of the explosive fragmentation of vesicular magma: Proceedings of the Royal Society of London A: Mathematical, Physical and Engineering Sciences, v. 466, p. 731–752.

Heap, M., Farquharson, J., Wadsworth, F., Kolzenburg, S., and Russell, J., 2015, Timescales for permeability reduction and strength recovery in densifying magma: Earth and Planetary Science Letters, v. 429, p. 223–233, doi:10.1016/j.epsl.2015.07.053.

Honarpour, M., Koederitz, F., and Herbert, A., 1986, Relative Permeability of Petroleum Reservoirs: Boca Raton, Florida, CRC Press Inc., 137 p.

Klug, C., and Cashman, K.V., 1996, Permeability development in vesiculating magmas: Implications for fragmentation: Bulletin of Volcanology, v. 58, p. 87–100, doi:10.1007/s004450050128.

Le Pennec, J.L., Hermitte, D., Dana, I., Pezard, P., Coulon, C., Cochemé, J.J., Mulyadi, E., Ollagnier, F., and Revest, C., 2001, Electrical conductivity and pore-space topology of Merapi Lavas: Implications for the degassing of porphyritic andesite magmas: Geophysical Research Letters, v. 28, p. 4283–4286, doi:10.1029/2001GL013401.

Martys, N.S., Torquato, S., and Bentz, D., 1994, Universal scaling of fluid permeability for sphere packings: Physical Review E: Statistical Physics, Plasmas, Fluids, and Related Interdisciplinary Topics, v. 50, p. 403–408, doi:10.1103/PhysRevE.50.403.

McKenzie, D., 1984, The generation and compaction of partially molten rock: Journal of Petrology, v. 25, p. 713–765, doi:10.1093/petrology/25.3.713.

Moyer, T.C., Geslin, J.K., and Flint, L.E., 1996, Stratigraphic relations and hydrologic properties of the Paintbrush Tuff nonwelded (PTn) hydrologic unit, Yucca Mountain, Nevada: U.S. Geological Survey Open-File Report 95-397, 151 p., doi:10.2172/374105.

Mueller, S., Melnik, O., Spieler, O., Scheu, B., and Dingwell, D.B., 2005, Permeability and degassing of dome lavas undergoing rapid decompression: An experimental determination: Bulletin of Volcanology, v. 67, p. 526–538, doi:10.1007/s00445-004-0392-4.

Mueller, S., Scheu, B., Spieler, O., and Dingwell, D.B., 2008, Permeability control on magma fragmentation: Geology, v. 36, p. 399–402, doi:10.1130/G24605A.1.

Norris, J.Q., Turcotte, D.L., and Rundle, J.B., 2015, A damage model for fracking: International Journal of Damage Mechanics, v. 24, p. 1227–1238, doi:10.1177/1056789515572927.

Okumura, S., and Sasaki, O., 2014, Permeability reduction of fractured rhyolite in volcanic conduits and its control on eruption cyclicity: Geology, v. 42, p. 843–846, doi:10.1130/G35855.1.

Okumura, S., Nakamura, M., Tsuchiyama, A., Nakano, T., and Uesugi, K., 2008, Evolution of bubble microstructure in sheared rhyolite: Formation of a channel-like bubble network: Journal of Geophysical Research, v. 113, B07208, doi:10.1029/2007JB005362.

Quane, S.L., and Russell, J.K., 2005, Welding: Insights from high-temperature analogue experiments: Journal of Volcanology and Geothermal Research, v. 142, p. 67–87, doi:10.1016/j.jvolgeores.2004.10.014.

Rintoul, M.D., 2000, Precise determination of the void percolation threshold for two distributions of overlapping spheres: Physical Review E: Statistical Physics, Plasmas, Fluids, and Related Interdisciplinary Topics, v. 62, p. 68–72, doi:10.1103/PhysRevE.62.68.

Rust, A., and Cashman, K., 2011, Permeability controls on expansion and size distributions of pyroclasts: Journal of Geophysical Research, v. 116, B11202, doi:10.1029/2011JB008494.

Saar, M.O., and Manga, M., 1999, Permeability-porosity relationship in vesicular basalts: Geophysical Research Letters, v. 26, p. 111–114, doi:10.1029/1998GL900256.

Scheidegger, A.E., 1963, The Physics of Flow through Porous Media: Toronto, Canada, University of Toronto Press, 353 p.

Torquato, S., 2013, Random Heterogeneous Materials: Microstructure and Macroscopic Properties: New York, Springer-Verlag, 703 p.

Tuffen, H., and Dingwell, D., 2005, Fault textures in volcanic conduits: Evidence for seismic trigger mechanisms during silicic eruptions: Bulletin of Volcanology, v. 67, p. 370–387, doi:10.1007/s00445-004-0383-5.

von Bargen, N., and Waff, H., 1986, Permeabilities, interfacial areas and curvatures of partially molten systems: Results of numerical computations of equilibrium microstructures: Journal of Geophysical Research, v. 91, p. 9261–9276, doi:10.1029/JB091iB09p09261.

Wadsworth, F.B., Vasseur, J., Aulock, F.W., Hess, K.U., Scheu, B., Lavallée, Y., and Dingwell, D.B., 2014, Nonisothermal viscous sintering of volcanic ash: Journal of Geophysical Research, v. 119, p. 8792–8804, doi:10.1002/2014JB011453.

Westrich, H.R., and Eichelberger, J.C., 1994, Gas transport and bubble collapse in rhyolitic magma: An experimental approach: Bulletin of Volcanology, v. 56, p. 447–458, doi:10.1007/BF00302826.

Wright, H.M., and Cashman, K.V., 2014, Compaction and gas loss in welded pyroclastic deposits as revealed by porosity, permeability, and electrical conductivity measurements of the Shevlin Park Tuff: Geological Society of America Bulletin, v. 126, p. 234–247, doi:10.1130/B30668.1.

Manuscript received 24 November 2015
Revised manuscript received 20 January 2016
Manuscript accepted 22 January 2016

Printed in USA